

## Nonsaturable Binding Indicates Clustering of Tau on the Microtubule Surface in a Paired Helical Filament-like Conformation\*

Received for publication, March 27, 2000, and in revised form, June 26, 2000  
Published, JBC Papers in Press, June 26, 2000, DOI 10.1074/jbc.M002590200

Michael Ackmann‡, Hans Wiech, and Eckhard Mandelkow§

From the Max-Planck-Unit for Structural Molecular Biology c/o DESY, Notkestrasse 85, D-22607 Hamburg, Germany

**Tau protein modulates microtubule dynamics and forms insoluble aggregates in Alzheimer's disease. Because there is a discrepancy between reported affinities of Tau to microtubules, we determined the interaction over a wide concentration range using a sensitive enzyme-linked immunosorbent assay. We found that the interaction is biphasic and not monophasic as assumed earlier. The first binding phase is typical for identical and noninteracting binding sites, with dissociation constants around 0.1  $\mu\text{M}$  and stoichiometries around 0.2 Tau/tubulin dimer. Surprisingly, the second phase is nonsaturable and shows a nearly linear increase in bound Tau versus free Tau for free Tau concentrations higher than 2  $\mu\text{M}$ . The slope is proportional to the microtubule concentration. From this we define an overloading parameter with values around 50  $\mu\text{M}$ . The influence of Tau isoform, phosphorylation, and dimerization on both phases was investigated. Remarkably the overloading of Tau on microtubules leads to a thioflavin S fluorescence increase reminiscent of that seen with Tau aggregated into Alzheimer paired helical filaments. Because polyanions stimulate Tau aggregation and because the C-terminal domain of tubulin is polyanionic, we suggest that an early conformational change in Tau leading to paired helical filament aggregation occurs right on the microtubule surface.**

Microtubules (MTs)<sup>1</sup> consist of tubulin with several types of MT-associated proteins (MAPs) attached. Because MAPs possess the ability to bind to MTs and to stimulate tubulin polymerization *in vitro*, they are believed to play an important role in the regulation of MT formation and stabilization *in vivo*. The neuronal MAPs, MAP2 and Tau, and the non-neuronal MAP4 belong to one family characterized by a domain of 3–4 internal repeats in the C-terminal half (Fig. 1); they have been well characterized at the biochemical level (for reviews see Refs. 1 and 2).

One of the neuronal MAPs in mammalian brain, Tau protein,

is normally found on axonal MTs and is the major component of paired helical filaments (PHFs) found in Alzheimer's disease brain. To understand the neurodegenerative process in which Tau changes from the MT bound form to the self-assembled form in PHFs, it is important to analyze the binding characteristics of Tau to MTs and how these are affected by changes inherent to pathological Tau. It has been speculated that a reduced affinity of Tau to MTs, the tracks of axonal transport, would cause the breakdown of MTs and hence have severe effects on axonal transport, resulting in a pathological state like Alzheimer's disease; this is consistent with the observation that Tau from Alzheimer brains no longer binds to MTs (3, 4). On the other hand, overexpression of binding-competent Tau could inhibit axonal transport by interfering with motor proteins (5).

A number of investigations on the binding of Tau to MTs have been reported (6–14). But a discrepancy between the results has persisted, presumably because of the different experimental approaches and different concentration ranges that were used. One approach was to vary the MT concentration and to leave the Tau concentration constant. For example, Butner and Kirschner (9) varied tubulin from 0.11 to 3.6  $\mu\text{M}$  at constant 2.4 nM <sup>35</sup>S-labeled Tau; Goode and Feinstein (12) varied tubulin from 0.01 to 40  $\mu\text{M}$  at constant 0.1 nM <sup>35</sup>S-labeled Tau. In these conditions the Tau concentration remained low compared with tubulin (<50-fold). The analysis of radiolabeled bound and free Tau separated by SDS-PAGE and subsequent fluorographic quantitation yielded an apparent dissociation constant ( $K_{\text{app}} = K_d/n$ ) but not the intrinsic dissociation constant ( $K_d$ ) and stoichiometry ( $n$ , number of Tau binding sites per tubulin dimer) separately. The  $K_{\text{app}}$  was reported to be around 0.11–0.16  $\mu\text{M}$  (9, 12).

Alternatively, one can leave the MT mass concentration constant and vary the Tau concentration; for example, in our previous work (11) tubulin was held constant at 30  $\mu\text{M}$  and Tau varied from 1 to 30  $\mu\text{M}$ ; Hong *et al.* (13) held tubulin constant at 3  $\mu\text{M}$  tubulin dimer and varied Tau from 0.2  $\mu\text{M}$  to 2  $\mu\text{M}$ . In these conditions the tubulin concentration remained in excess over Tau. Bound and free Tau were separated by SDS-PAGE followed by quantitation of Coomassie stained gels or after performing a quantitative radioimmunoassay. This approach yielded the intrinsic dissociation constant and stoichiometry separately (Ref. 11,  $K_d = 1.1 \mu\text{M}$ ,  $n = 0.46$ ; Ref. 13,  $K_d = 0.039 \mu\text{M}$ ,  $n = 0.41$ ). Thus there was a reasonable agreement in stoichiometries but not in the  $K_d$  values.

The affinity of Tau for MTs is important when assessing its possible biological and pathological roles. The tubulin concentration in cells is on the order of 40  $\mu\text{M}$  (15); the reported concentrations of Tau are variable (depending on cell type or tissue sample) but are substantially lower than tubulin (7, 8, 16). In addition Tau can exert its MT-stabilizing function even

\* This work was supported by the Deutsche Forschungsgemeinschaft. The costs of publication of this article were defrayed in part by the payment of page charges. This article must therefore be hereby marked "advertisement" in accordance with 18 U.S.C. Section 1734 solely to indicate this fact.

‡ This work was done in part as a doctoral thesis.

§ To whom correspondence should be addressed. Tel.: 49-40-89982810; Fax: 49-40-89716822; E-mail: mand@mpasmb.desy.de.

<sup>1</sup> The abbreviations used are: MT, microtubule; ELISA, enzyme linked immunosorbent assay; FTDP-17, frontotemporal dementia and parkinsonism linked to chromosome 17; MAP, microtubule-associated protein; PHF, paired helical filament; PIPES, 1,4-piperazinediethane sulfonic acid; PKA, cAMP-dependent protein kinase; ThS, thioflavin S; PAGE, polyacrylamide gel electrophoresis.

at very low concentrations (17). The question has recently gained particular attention with the discovery of Tau mutants related to certain frontotemporal dementias (FTDP-17) in which Tau aggregates into PHFs similar to those of Alzheimer's disease (18, 19). One possible explanation of the pathology could be the loss of MT affinity, and therefore several authors reported comparative studies of the ability of Tau mutants to stimulate MT assembly and to bind to MTs (13, 20, 21).

To address these questions we have recently developed a sensitive and specific enzyme linked immunosorbent assay (ELISA) for Tau. This enabled us to determine Tau in the MT binding assay over a wider range of concentrations than previously possible. We found that the binding of Tau to MTs is not monophasic, as assumed in earlier studies but contains at least two phases. Unexpectedly, the second phase is not saturable within our concentration range and results in high apparent concentrations of Tau on the MT surface. These findings prompted us to ask whether there is a relationship between the binding of Tau to MTs and aggregation of Alzheimer PHFs. The pathological aggregation is known to be stimulated by polyanions, including acidic peptides such as poly-Glu (22). Tubulin has a highly acidic C-terminal domain to which Tau and related MAPs bind (14, 23–27). It is therefore conceivable that high concentrations of Tau on the MT surface could initiate PHF aggregation. This issue was addressed using our recently developed thioflavin S assay (22). Finally, we used the ELISA binding assay to ask how posttranslational modifications of Tau would affect its affinity for MTs (28), in particular phosphorylation (because this is increased in pathological conditions) and dimerization (because Tau dimers constitute building blocks for PHF aggregation; Ref. 29).

## MATERIALS AND METHODS

### Proteins and Chemicals

Bovine brain tubulin was purified by MAP-depleting steps and phosphocellulose chromatography (30). Human Tau23 (hTau23) and Tau40 (hTau40) were expressed in *Escherichia coli* as described (10). The numbering of amino acids refers to the isoform hTau40 containing 441 residues (31). The proteins were expressed and purified, making use of the heat stability followed by fast protein liquid chromatography on Mono S (Amersham Pharmacia Biotech) (11). The purity of the proteins was analyzed by SDS-PAGE. Tau concentrations were determined in ELISA with His-tagged hTau40 as a standard, which had been previously weighed out. Other protein concentrations were determined by the BCA assay using bovine serum albumin as standard.

Phosphorylation of human Tau40 by cAMP-dependent protein kinase (PKA) was performed in conditions where Ser<sup>214</sup> becomes uniquely and quantitatively phosphorylated (32). The incorporation of phosphate was quantified by the addition of [ $\gamma$ -<sup>32</sup>P]ATP to the phosphorylation mixture, separation on SDS-PAGE, and scintillation counting of the band with phosphorylated Tau. The dimerization of Tau was achieved by allowing hTau23 to become air-oxidized in the absence of dithiothreitol; dimers are formed quantitatively by disulfide cross-linking at the single cysteine Cys<sup>322</sup> (33).

The monoclonal antibodies Tau-1 (epitope, amino acids 193–204 in unphosphorylated form; Ref. 34) and Tau-R4 (epitope, amino acids 344–351) were used as "capturing" antibodies for the Tau-ELISA. They were purified over a protein G column from a cell culture supernatant or ascites fluid. For detection antibodies, polyclonal rabbit sera SA4470 (epitope, amino acids 1–14), SA5981 (epitope, amino acids 142–154), and SA4478 (epitope, amino acids 428–441) were raised against target peptides and obtained from Eurogentec, Inc. (see Fig. 1). These sera were affinity purified using hTau40 conjugated to NHS-activated Sepharose (Amersham Pharmacia Biotech) and biotinylated according to the suppliers protocol.

Taxol, heparin (average molecular weight of 6000), and ThS were supplied by Sigma. All other materials used were of reagent grade.

### Tau-ELISA

An enzyme-linked immunosorbent assay (sandwich ELISA) was performed as follows. All incubations described below were done at 20 °C,

and between all steps the plate was washed three times with 150  $\mu$ l of TTBS (100 mM Tris-HCl, pH 7.5, 150 mM NaCl, 0.1% Tween 20)/well. The monoclonal anti-hTau antibodies Tau-1 and Tau-R4 were used together as capturing antibodies by coating an Immuno-plate (Greiner, Frickenhausen, Germany) at 20  $\mu$ g/ml each in 100  $\mu$ l coating buffer (12 mM Na<sub>2</sub>CO<sub>3</sub>, 36 mM NaHCO<sub>3</sub>, pH 9.6)/well for 1 h (phosphorylation of Tau by PKA did not influence the binding capability of these antibodies; data not shown). Unspecific binding sites were saturated by incubation with 150  $\mu$ l of blocking buffer (10% fetal calf serum, 0.25% gelatin, 60 mM Tris-HCl, pH 7.5, 225 mM NaCl, 0.1% Tween 20)/well for 1 h. For detection of captured Tau a combination of protein affinity purified biotinylated polyclonal anti-hTau antibodies (SA4470, SA5981, and SA4478) was added 2-fold concentrated in 50  $\mu$ l/well. Then a 50- $\mu$ l sample (Tau concentration between 30 and 300 pM or for hTau40 1.35 to 13.5 pg/ $\mu$ l) diluted in Combi Blotto was applied, and the plate was incubated for 16 h. Amplification was obtained by binding of 100  $\mu$ l of horseradish peroxidase-conjugated streptavidin (Vector Laboratories, Burlingame, CA; 1:2000 diluted in TTBS) for 30 min, additional biotinylation of the formed immune complex for 10 min by 100  $\mu$ l of tyramide biotin (tyramide signal amplification (TSA)-indirect kit; NEN Life Science Products; 1:300 diluted in TTBS), and subsequent binding of 100  $\mu$ l of horseradish peroxidase-conjugated streptavidin (1:5000 diluted in TTBS) for 30 min. After incubation with 100  $\mu$ l of substrate solution (7 mM *o*-phenylenediamine, 55 mM citronic acid, 90 mM Na<sub>2</sub>HPO<sub>4</sub>, 0.13% H<sub>2</sub>O<sub>2</sub>, pH 4.5) in 5 min a chromophor was formed. The reaction was then stopped by addition of 50  $\mu$ l of 1 M H<sub>2</sub>SO<sub>4</sub>, and the intensity of the color reaction was measured as the difference between the absorption at 490 nm and the absorption at 410 nm. This value was proportional to the amount of Tau in a range between 15 and 500 pM (for hTau40 between 0.675 and 22.5 pg/ $\mu$ l).

### MT Binding Assay

**Preparation of Tubulin Stock Solution**—Purified tubulin (140–230  $\mu$ M tubulin dimer) in RB buffer (100 mM Na-PIPES, pH 6.9, 1 mM EGTA, 1 mM MgCl<sub>2</sub>, 1 mM dithiothreitol) was centrifuged at 62,000  $\times$  g for 8 min and 4 °C to remove aggregates. Stock solutions were added to the supernatant to obtain RB\* buffer (100 mM Na-PIPES, pH 6.9, 1 mM EGTA, 1 mM MgCl<sub>2</sub>, 1 mg/ml bovine serum albumin, 1 mM GTP, 1 mM phenylmethylsulfonyl fluoride, 50  $\mu$ M taxol, 1 mM dithiothreitol). Tubulin was allowed to polymerize for 30 min at 37 °C. The MT concentration (tubulin dimer concentration) was then adjusted to obtain a 10-fold stock solution with respect to the final concentration in the binding assay. After centrifugation at 62,000  $\times$  g for 8 min and 25 °C the supernatant was discarded and the MT pellet was suspended by adding the original volume (before the centrifugation) of RB\* buffer. This 10 $\times$  MTs stock solution was stored at 25 °C for not more than 12 h. In this paper the concentration of MTs is defined as the concentration of tubulin dimers that are polymerized by 50  $\mu$ M taxol.

**Preparation of Tau Protein Dilution Series**—Purified Tau protein in RB\* buffer was centrifuged at 62,000  $\times$  g for 8 min and 25 °C. The supernatant was used for serial dilutions in RB\* buffer with a final volume of 60  $\mu$ l spanning a concentration range between 1/10 and 10 times the MT concentration (tubulin dimer concentration) used in the binding assay. Of the 60- $\mu$ l volume 15  $\mu$ l each were used to determine the total amount of Tau using the Tau-ELISA.

**Binding Assay**—The binding assay was performed in RB\* buffer. 5  $\mu$ l of the 10-fold tubulin stock solution were added to the remaining 45  $\mu$ l of Tau protein solution (concentration as indicated), and the samples were incubated for 20 min at 37 °C. The suspension was fractionated into supernatants (unbound Tau, 25  $\mu$ l for the Tau-ELISA; the remaining supernatant was discarded) and MT pellets (bound Tau) by centrifugation for 8 min at 62,000  $\times$  g at 25 °C. Centrifugation over 50% sucrose cushion (to remove spurious unbound Tau) did not change the values. The resulting pellets were not washed to maintain the equilibrium, resuspended in 50  $\mu$ l RB\* buffer with 500 mM NaCl, and incubated for 1 h at 0 °C to disassemble the MTs and release bound Tau. The protein concentration of Tau in the resuspended pellet fractions (bound Tau) and supernatants (free Tau), and the total amount was determined by the Tau-ELISA. For this purpose the samples were diluted to get into the linear assay range. The NaCl in the resuspended pellet fractions did not influence the ELISA result because the samples were diluted, and the ELISA sample incubation buffer (under "Tau-ELISA") itself contained 225 mM NaCl.

### Data Reduction and Interpretation

In our experiments we used a fixed concentration of MTs (3 or 20  $\mu$ M) and added increasing concentrations of Tau. [Tau]<sub>bound</sub> was plotted

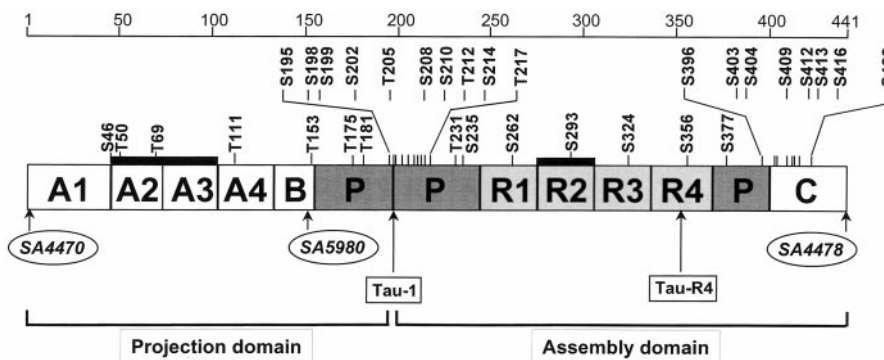


FIG. 1. **Diagram of Tau, phosphorylation sites, and epitopes of capturing and detection antibodies used in Tau-ELISA.** The bar shows hTau40, the largest Tau isoform in the human central nervous system. The C-terminal half contains up to four repeats (*R1–R4*) embedded in proline-rich domains (*P*) that are responsible for MT binding and PHF aggregation. Some known phosphorylation sites are marked on top. Inserts *A2* and *A3* and repeat *R2* may be absent because of alternative splicing. Capturing antibodies of the ELISA are shown in rectangles (*tau-1* and *tau-R4*), and detection antibodies are in ovals (*SA4470*, *SA5980*, and *SA4478*). Notice that the antibodies recognize sites that are common to all Tau isoforms so that the ELISA signal is independent of the isoform analyzed.

versus  $[\text{Tau}]_{\text{free}}$  and fitted by nonlinear regression using the standard binding equation for a macromolecule with equivalent and noninteracting ligand binding sites (Equation 1), or using an equation with two binding terms (Equation 2). The first term of Equation 2 represents equivalent and noninteracting ligand binding sites (as in Equation 1), and the second term represents an accumulation of bound Tau proportional to the concentrations of tubulin and free Tau. As a control for the measurement the sum of free Tau and bound Tau should be total Tau for each data triplet. Only data triples that fulfilled this quality criterion were evaluated.

$$[\text{Tau}]_{\text{bound}} = \frac{n \cdot [\text{MT}] \cdot [\text{Tau}]_{\text{free}}}{K_d + [\text{Tau}]_{\text{free}}} \quad (\text{Eq. 1})$$

$$[\text{Tau}]_{\text{bound}} = \frac{n \cdot [\text{MT}] \cdot [\text{Tau}]_{\text{free}}}{K_d + [\text{Tau}]_{\text{free}}} + \frac{1}{p} \cdot [\text{MT}] \cdot [\text{Tau}]_{\text{free}} \quad (\text{Eq. 2})$$

The monophasic Equation 1 saturates at  $[\text{Tau}]_{\text{bound}} = n [\text{MT}]$  for high Tau concentrations, yielding the stoichiometry  $n = [\text{Tau}]_{\text{bound}}/[\text{MT}]$ . 50% of the maximum binding is reached when  $[\text{Tau}]_{\text{free}}$  equals the  $K_d$ . Equation 2 was applied for a biphasic analysis of the binding data, resulting in the values for the dissociation constants ( $K_d$ ), the stoichiometry ( $n$ ), and the overloading parameter ( $p$ ). Note that  $p$  describes the rising branch of a second phase. It is formally reminiscent of a  $K_d$  value describing a weak affinity of Tau, except that no saturation is observed.

For comparison, we note that other authors (9, 12) titrated increasing MT concentrations against a fixed (and very low) concentration of Tau. For this case the fraction of bound Tau,  $[\text{Tau}]_{\text{bound}}/[\text{Tau}]_{\text{tot}}$ , was plotted against MTs,  $[\text{MT}]$ . For this case, both sides of Equation 1 are divided by  $[\text{Tau}]_{\text{tot}}$ .

$$\frac{[\text{Tau}]_{\text{bound}}}{[\text{Tau}]_{\text{tot}}} = \frac{n \cdot [\text{MT}] \cdot [\text{Tau}]_{\text{free}}}{(K_d + [\text{Tau}]_{\text{free}}) \cdot [\text{Tau}]_{\text{tot}}} \quad (\text{Eq. 3})$$

For high  $[\text{MT}]$ , the curve tends to  $[\text{Tau}]_{\text{bound}}/[\text{Tau}]_{\text{tot}} = 1$  (i.e. all Tau bound to MTs), the 50% point is reached at  $[\text{Tau}]_{\text{bound}}/[\text{Tau}]_{\text{tot}} = [\text{Tau}]_{\text{free}}/[\text{Tau}]_{\text{tot}} = 0.5$ , implying  $n [\text{MT}] = (K_d + [\text{Tau}]_{\text{free}})$ . Because  $[\text{Tau}]_{\text{free}} \ll K_d$  under the experimental conditions, this yields  $[\text{MT}] = K_d/n = K_{\text{app}}$ . In other words, the experiment yields the apparent dissociation constant ( $K_{\text{app}} = K_d/n$ ) but not the intrinsic dissociation constant and stoichiometry separately.

#### Fluorescence Spectroscopy

Fluorescence of thioflavin S was measured with a Fluoroskan Ascent microtiter plate reader (Labsystems, Helsinki, Finland) with an excitation filter of 440 nm (bandwidth, 10 nm) and an emission filter of 510 nm (bandwidth, 10 nm) in a 384-well plate. Measurements were carried out at room temperature in ammonium acetate 50 mM, pH 7.0, with 10  $\mu\text{M}$  ThS. Background fluorescence and light scattering of the sample without thioflavin S was subtracted if necessary.

#### Electron Microscopy

Protein solutions diluted to 1–10  $\mu\text{M}$  protein were placed on 600-mesh carbon-coated copper grids for 1 min and negatively stained with 2% uranyl acetate for 45 s. The specimens were examined in a Philips CM12 electron microscope at 100 kV.

## RESULTS

**Measuring the Tau Concentration by ELISA**—One problem in measuring Tau-MT interactions is the limited concentration range of the different assays used because the analysis of bound and free Tau was performed on SDS-PAGE followed by densitometric determination of a Coomassie-stained band or after performing a quantitative radioimmunoassay. Therefore, a sandwich ELISA was developed using two monoclonal anti-hTau antibodies, Tau-1 (34) and Tau-R4, as capturing antibodies. For detection of captured Tau a combination of protein affinity purified biotinylated polyclonal anti-hTau antibodies, SA4470 (epitope, amino acids 1–14), SA5981 (epitope, amino acids 142–154), and SA4478 (epitope, amino acids 428–441), was applied (Fig. 1) and detected by peroxidase-conjugated streptavidin. Amplification was obtained by additional biotinylation of the immune complex by tyramide-biotin and subsequent binding of peroxidase-conjugated streptavidin (35). After incubation with a substrate, a chromophore was formed where the intensity of the color reaction was proportional to the amount of Tau (Fig. 2).

We obtained a linear calibration curve of the Tau-ELISA between 15 and 500 pM (for hTau40 this corresponds to 0.675–22.5 ng/ml). The detection limit of the assay was  $\sim 10$  pM. To estimate the absolute amount of purified Tau we used His-tagged hTau40 as a standard in the ELISA, which was previously weighed out. In cases where the concentration of Tau was too high, the samples were measured after serial dilutions until the linear range of the Tau-ELISA was reached. In summary, the Tau-ELISA fulfilled all the criteria for measuring the Tau concentration in a sensitive and specific way. These features were important for the evaluation and validation of Tau binding to MTs.

**MT Binding of Tau Isoforms, Tau Dimers, and Phosphorylated Tau**—The binding of human Tau40 (largest isoform in the central nervous system) and hTau23 (smallest isoform) to taxol-stabilized MTs was analyzed using the Tau-ELISA to determine the bound and free fractions of Tau. In addition we determined the effects of Tau phosphorylation by PKA and Tau dimerization. The studies were done at two concentrations of polymerized tubulin, 3 and 20  $\mu\text{M}$  (dimer concentration). Fig. 3 shows a set of binding curves obtained with hTau23 at 3  $\mu\text{M}$  MTs. The binding curves are highly reproducible, even between different Tau preparations. One can recognize two phases, an initial rising phase that tends to saturation between 10 and 20  $\mu\text{M}$  free Tau and that is superseded by a second linearly rising phase with no observable saturation even at 120  $\mu\text{M}$  total Tau. Fig. 4a shows an analogous experiment with hTau40 at a

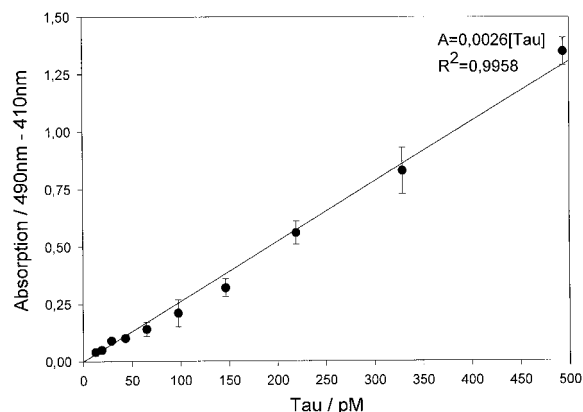


**FIG. 2. Standard curve for Tau-ELISA.** The absorption difference ( $A_{490} - A_{410}$ ) is plotted against the hTau40 concentration. The error of the data points represents a probability interval of 95%. The equation of the linear regression (line) yields a value of  $R^2 = 0.9958$ . The assay was performed with the conditions that the absorption difference ( $A_{490} - A_{410}$ ) of the sample diluent was  $<0.06$  (minimal signal) and that the absorption difference of the 400 pM standard was around 1.0 (nearly maximal signal in the linear range). The detection limit was  $10 \pm 2$  pM and was calculated as the mean of five determinations of the sample diluent. The recovery of Tau spiked in different samples was  $95 \pm 4\%$  showing a coefficient of variation on the mean final concentration below 10% after serial  $\frac{1}{2}$  dilutions. The intra-assay coefficient of variation on three parallel determinations of five samples and two standards was below 12%. Error bars show 2-fold S.E.

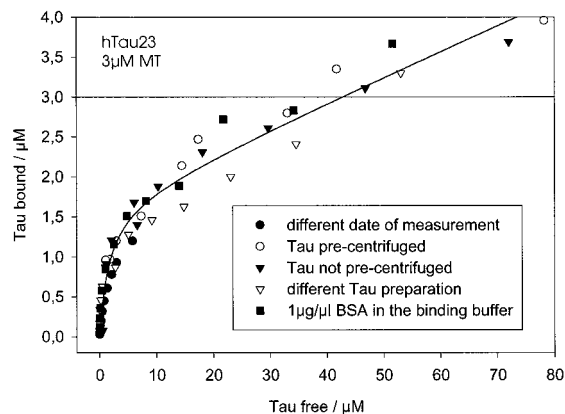


**FIG. 3. Tau-MT binding curves in different conditions.** Bound hTau23 is plotted versus free hTau23 at a constant total MT concentration of  $3 \mu\text{M}$  tubulin dimers (indicated by the horizontal line). Note the biphasic binding behavior (approach to saturation in the first phase, followed by linear increase). The binding curve was reproducible under various conditions (different date of measurement; Tau precentrifuged or not, different Tau preparations,  $1 \mu\text{g}/\mu\text{l}$  bovine serum albumin in the binding buffer).

higher MT concentration ( $20 \mu\text{M}$ ) with the same biphasic binding behavior. In Fig. 4b the same data are plotted as in Fig. 4a but leaving out the concentration range above  $20 \mu\text{M}$  free Tau. In this case the data appear to agree reasonably well with a monophasic binding curve (see Equation 1) saturating around  $8 \mu\text{M}$  bound Tau.

However, the monophasic data reduction is clearly too limited to explain the data, as seen by the continuous rise at higher concentrations. It would be tempting to apply a more general fit based on two types of equivalent and noninteracting ligand binding sites, one weak and one strong. If this is done one obtains poor fits, obviously because no saturation is visible for the weak binding phase. We therefore decided to allow the second term to be linear, as suggested by the available data (see Equation 2). In this case the strongly binding phase yields  $K_d = 0.075 \mu\text{M}$  for hTau40 and  $0.450 \mu\text{M}$  for hTau23, with comparable stoichiometries ( $n = 0.20$  and  $0.26$ ; Table I). These

$K_d$  values are about 5–10-fold lower than those determined by densitometry of SDS gels (11), but they are in good agreement with those of other authors (9, 12). The stoichiometries are also 2-fold lower than before, suggesting one Tau molecule for every 4–5 tubulin dimers or roughly one of the repeated motifs of Tau ( $\sim 31$  residues; Fig. 1) for every tubulin dimer.

If our data in Fig. 4a are fitted with a monophasic binding curve (Equation 1 or first term in Equation 2), they yield a dissociation constant between  $0.270$  and  $3.1 \mu\text{M}$  and a stoichiometry between  $0.32$  and  $0.64$  for the evaluation range  $0$ – $10 \mu\text{M}$  and  $0$ – $20 \mu\text{M}$  free Tau, respectively. This is in agreement with the results obtained earlier by densitometry of SDS gels in the same limited concentration range (10, 11), shown for comparison in Fig. 4a. In the same ranges the biphasic fit (Equation 2) yields a value for  $K_d$  between  $0.019$  and  $0.036 \mu\text{M}$  and a value for  $n$  between  $0.15$  and  $0.18$ , respectively. Thus, in contrast to the biphasic fit, the monophasic fit parameters, especially the dissociation constant, depend strongly on the selected evaluation range and differ from the first phase parameters of the biphasic fit. In general, the monophasic fit parameters for biphasic data become more similar to the biphasic fit parameters at lower evaluated Tau free concentrations.

The fact that the binding curves at higher concentrations are linear means that a constant fraction of added Tau becomes bound to the MTs while the rest remains in solution. Moreover, the bound fraction is roughly proportional to the MT concentration. This is illustrated in Fig. 4c where the y axis is on a logarithmic scale. The two binding curves were obtained at two different MT concentrations ( $3$  and  $20 \mu\text{M}$ ), and their ratio for bound Tau remains roughly constant through most of the range of free Tau. Thus the slope of the binding curves can be described as  $(1/p)[\text{MT}]$ , so that the parameter  $p$  becomes independent of the MT concentration. We can interpret the situation in terms of “overloading” the MT surface. Two mechanisms can be visualized. Already bound Tau molecules could cover up neighboring binding sites and thus inhibit newcomers from binding; these will force their way in only at higher concentration. This “parking problem” was analyzed in detail elsewhere (36); it would eventually lead to full saturation of all available binding sites at sufficiently high ligand concentrations. A second process is that at high local concentrations Tau associates with itself on the MT surface. In this case one would expect the second phase to be proportional to the MT concentration, as observed. We note that formally the linear increase in the weak binding phase is comparable with the initial part of a normal binding curve for very high  $K_d$  values. Thus  $p$  can be regarded as a kind of dissociation constant for overloading. For hTau40,  $p$  equals  $45 \mu\text{M}$ , for hTau23 the value is comparable,  $59 \mu\text{M}$  (Table I). This means that the two Tau isoforms differ mainly in their first phase binding constant but not so much in their stoichiometry and overloading parameter.

On the basis of the foregoing analysis we wanted to test how posttranslational modifications affect the binding parameters. Phosphorylation is perhaps the best characterized modification because it appears to regulate the behavior of Tau and its affinity for MTs both in physiological and pathological conditions. Tau contains many potential phosphorylation sites but most of these have only a moderate effect on Tau-MT interactions and consequently on MT dynamics. Exceptions to this rule are the sites affected by kinases PKA and MARK (37, 38). We therefore phosphorylated hTau40 with PKA because in this case the critical residue (Ser<sup>214</sup>) can be phosphorylated uniquely and to  $\sim 100\%$ . As shown earlier, this leads to the loss of both the MT binding and the Tau-Tau interactions in PHF assembly (32). Fig. 5a shows the results of the binding assay; the most striking difference is the stoichiometry, which drops

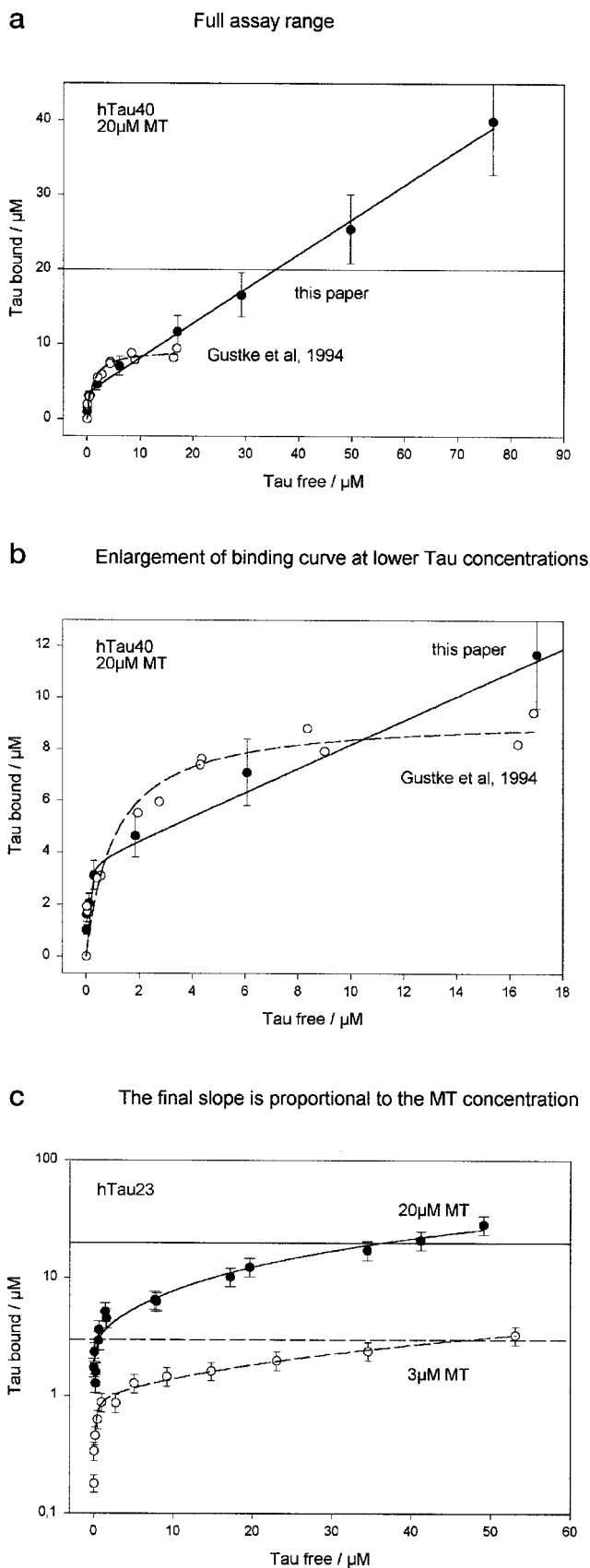


**FIG. 4. Analysis of the binding of Tau to MTs.** *a*, full assay range. Bound hTau40 is plotted versus free hTau40 at a constant total MT concentration of 20  $\mu\text{M}$  tubulin dimers (indicated by the horizontal line). Data in this paper (biphasic fit, filled circles and solid line) are compared with the data of Gustke *et al.* (Ref. 11; open circles, dashed line, monophasic fit; data rescaled from 30 to 20  $\mu\text{M}$  tubulin dimers). Both data sets are similar in their common range (up to  $\sim 18$   $\mu\text{M}$  free Tau),

**TABLE I**  
*Tau-MT binding parameters*

The parameters  $K_d$  (dissociation constant),  $n$  (stoichiometry of the first phase), and  $p$  (overloading parameter) were obtained from the data by a biphasic fit using Equation 2 (see "Materials and Methods").

	$K_d/\mu\text{M}$	$n$	$p/\mu\text{M}$
hTau40	$0.075 \pm 0.030$	$0.20 \pm 0.05$	$45 \pm 12$
hTau40p (PKA)	$0.100 \pm 0.050$	$0.03 \pm 0.01$	$71 \pm 20$
hTau23	$0.450 \pm 0.150$	$0.26 \pm 0.05$	$59 \pm 21$
hTau23-Dimer	$0.050 \pm 0.015$	$0.40 \pm 0.05$	$50 \pm 13$

7-fold (from 0.20 to 0.03; Table I), whereas the tight binding  $K_d$  remains comparable. The overloading parameter also increases by  $\sim 60\%$  (from 45 to 71  $\mu\text{M}$ ), indicating less accumulation of Tau on the MT surface during the second weak binding phase.

A second important modification is the dimerization of Tau by oxidation, which leads to the formation of disulfide bridges between Cys<sup>322</sup> on two molecules and thus to dimerization. Such Tau dimers from the building blocks for PHF aggregation (33). In this case the response to modification differs noticeably from that of phosphorylation (Fig. 5*b*); dimerization tightens the first phase binding almost by an order of magnitude ( $K_d$  drops from 0.450 to 0.050  $\mu\text{M}$ ), the stoichiometry increases by 50% (from 0.26 to 0.40), but the overloading parameter shows little change (from 59 to 50  $\mu\text{M}$ ; Table I). The data support the view that two covalently linked Tau molecules bind jointly and cooperatively to the MT surface.

*Nature of the Nonsaturable Binding of Tau to MTs*—If Tau indeed accumulates loosely on the MT surface, it should be possible to image this by electron microscopy. However, Tau is notorious for its poor visibility (39–43). This is consistent with its hydrophilic nature and intrinsic "natively unfolded" structure; in addition Tau tends to dissociate from the MT during the staining procedure. It means that the remaining Tau does not generate sufficient contrast in negative stain, which is illustrated in Fig. 6 for undecorated and Tau-decorated MTs. Some protrusions can be detected on the decorated MTs, but they are neither periodic nor consistent enough for interpretation. This is in clear contrast to MTs decorated with the motor protein kinesin, which has a globular structure and binds periodically (44).

On the other hand the high local concentration of Tau on the MT surface is intriguing in the light of the tendency of Tau to aggregate into Alzheimer PHFs in the presence of polyanions. Potent PHF inducers include the polyanions heparan sulfate, RNA, and poly-Glu (45–47). The C-terminal region of tubulin on the surface of MTs (to which Tau binds) is unusually acidic and can be further potentiated by enzymatic polyglutamylation (48, 49). We therefore suspected that Tau might adopt an association or conformation reminiscent of that in PHFs. This

but the increase of bound Tau at higher concentrations was outside the range of Gustke *et al.* (11). There is no sign of saturation at high Tau concentrations. The slope of the curve is roughly  $\frac{1}{2}$  (but proportional to the MT concentration; see panel *c*), i.e.  $\sim \frac{1}{3}$  of added Tau becomes bound, and  $\sim \frac{2}{3}$  remains free. Error bars show 2-fold S.E. *b*, enlargement of binding curve at lower Tau concentrations. Comparison of present data (filled circles) with those of Gustke *et al.* (Ref. 11; open circles). Note that in the restricted range of low Tau concentrations, both data sets seem roughly compatible with the assumption of monophasic binding (dashed curve). The initial binding of the biphasic fit yields a  $K_d$  value of 0.075  $\mu\text{M}$  and a stoichiometry of  $n = 0.20$ , whereas the monophasic fit in the range shown here yields an apparent  $K_d$  of 3.1  $\mu\text{M}$  and stoichiometry of  $n = 0.64$ . Error bars show 2-fold S.E. *c*, the final slope is proportional to the MT concentration. Binding curves and biphasic fits of hTau23 at a constant total MT concentrations (indicated by the horizontal lines) of 20  $\mu\text{M}$  (filled circles, solid line) or 3  $\mu\text{M}$  tubulin dimers (open circles, dashed line). The final slope is proportional to the MT concentration so that the slopes are similar when y axis is on a logarithmic scale. Error bars show 2-fold S.E.

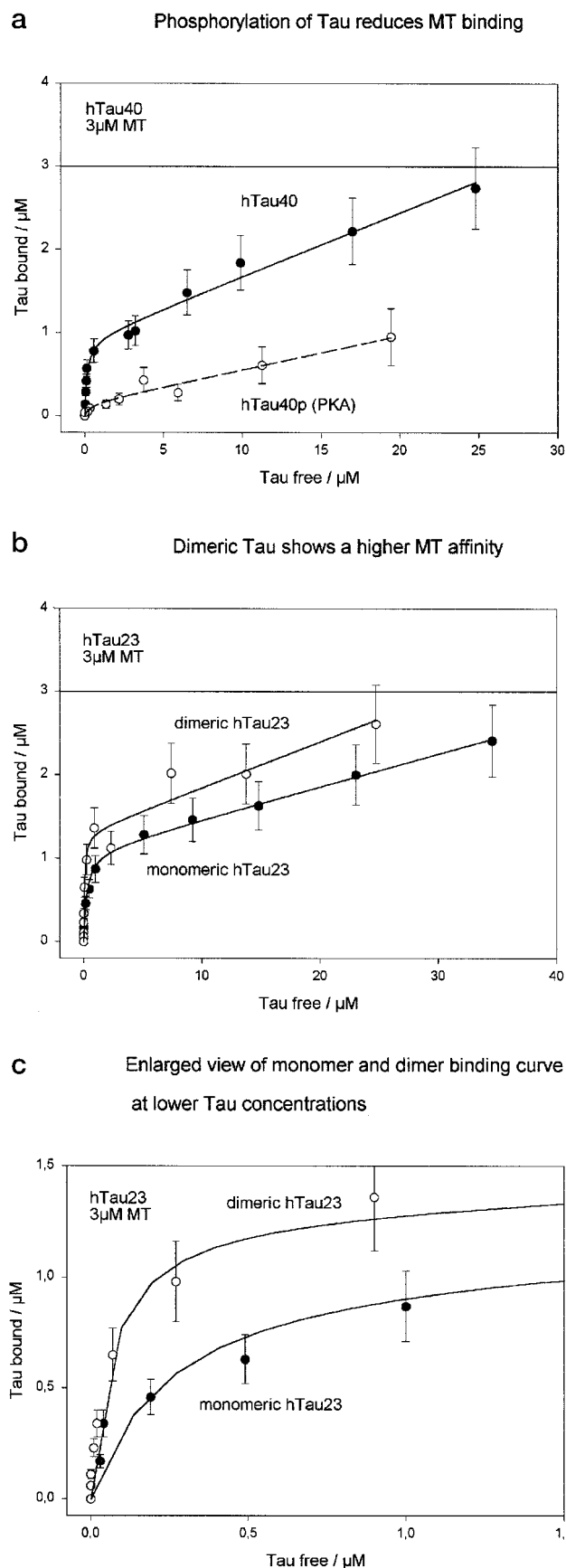


FIG. 5. *a*, phosphorylation of Tau reduces MT binding. Binding curves and biphasic fits of unphosphorylated hTau40 (filled circles, solid line) and hTau40 phosphorylated with PKA (open circles, dashed line). The total microtubule concentration was 3  $\mu\text{M}$  tubulin dimers (horizontal line). The incorporation was 1 phosphate/Tau molecule at Ser<sup>214</sup> (61).

was tested using a recently developed assay for PHF aggregation, based on the increased fluorescence of the dye thioflavin S. This assay was applied to MTs preincubated with different concentrations of hTau23 for 7 h at 37  $^{\circ}\text{C}$  (Fig. 7). When the proteins were added to the dye-containing buffer (background level, 0.8 units), the fluorescence changed within a few minutes as the dye associated. Tau alone at 50  $\mu\text{M}$  caused a noticeable drop in fluorescence (up to  $-40\%$ , depending on concentration). MTs alone caused only a slight change above background ( $\sim +10\%$ ), but Tau plus MTs induced a pronounced increase (up to  $+140\%$ , depending on the Tau concentration), which was even more pronounced when comparing it with the lower level of Tau alone. As a control, PHFs polymerized from hTau23 with heparin increased the level by  $\sim 80\%$ . These results are consistent with the view that the accumulation of Tau on the MT surface induces a state that is reminiscent of PHFs, which neither Tau nor MTs alone can achieve. This state could be equivalent to an incipient nucleation of PHF-like oligomers of Tau.

#### DISCUSSION

*Tau-MT Binding Parameters*—The Tau-MT interaction has been the topic of several studies. The reasons are that Tau is the major MAP in neuronal axons and plays a major role in neurite outgrowth, axonal stability, and maintenance of MTs as the tracks of axonal transport. From a biomedical point of view, Tau has been a target of research because it forms the backbone of the PHFs of Alzheimer's disease and related dementias. Some dementias can in fact be traced back to mutations in the Tau gene on chromosome 17, *e.g.* a group of frontotemporal dementias termed FTDP-17 (19, 50). Besides forming insoluble aggregates, the pathological Tau is also highly phosphorylated and can no longer bind and stabilize MTs (3, 4, 51). These findings made biochemical parameters such as  $K_d$  values important for understanding the perturbation in the MT cytoskeleton of neurons. There is a consensus that four-repeat Tau isoforms bind MTs better than three-repeat isoforms (because the repeats together with the flanking regions represent the MT binding site (9, 11, 12), that phosphorylation tends to reduce the affinity between Tau and MTs (although the magnitude of the effect varies, depending on the phosphorylation sites), and that the mutations of FTDP-17 tend to change the affinity as well, although here the effect is less clear cut because there is also a shift in the isoform expression pattern (13).

Considering the implications of Tau-MT interactions, the affinities reported in the literature vary over an uncomfortably large range, from below 0.1  $\mu\text{M}$  to above 1  $\mu\text{M}$ , *i.e.* more than an order of magnitude. With this range of experimental uncertainty it would be difficult to assess the impact of subtle

Phosphorylation reduces the binding mainly by a 7-fold decrease of the stoichiometry in the initial binding phase ( $n =$  from 0.20 to 0.03; Table I) and a  $\sim 2$ -fold decrease in the slope of the second phase ( $p =$  from 45 to 71  $\mu\text{M}$ ), whereas the dissociation constant is nearly unchanged ( $K_d =$  from 0.075 to 0.100  $\mu\text{M}$ ). Error bars show 2-fold S.E. *b*, dimeric Tau shows a higher MT affinity. Binding curves and biphasic fits of hTau23-monomer and hTau23-dimer (cross-linked at Cys<sup>322</sup>) at a constant total MT concentration (3  $\mu\text{M}$  tubulin dimer, horizontal line). Compared with the monomer the dimer shows enhanced binding seen in a 9-fold lower  $K_d$  in the first binding phase (from 0.450  $\mu\text{M}$  for the monomer to 0.050  $\mu\text{M}$  for the dimer; Table I) and a slightly higher value for  $n$  (0.26 for the monomer, 0.40 for the dimer), whereas  $p$  is nearly unchanged (59  $\mu\text{M}$  for the monomer, 50  $\mu\text{M}$  for the dimer). Error bars show 2-fold S.E. *c*, enlarged view of monomer and dimer binding curve at lower Tau concentrations. Note that in the restricted range of Tau the curves seem to approach saturation. A monophasic fit in this concentration range would yield apparent values of  $K_d = 0.530 \mu\text{M}$ ,  $n = 0.48$  for the monomer and  $K_d = 0.078 \mu\text{M}$ ,  $n = 0.47$  for the dimer. Error bars show 2-fold S.E.

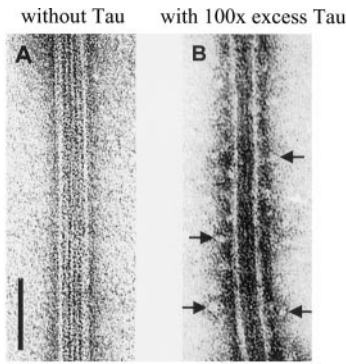


**FIG. 6. Negative stain electron microscopy of MTs without or with Tau.** *A*, undecorated MT without Tau, showing largely smooth walls and clear longitudinal striations because of the protofilaments. *B*, MT incubated for 10 min at 37 °C with 30  $\mu\text{M}$  hTau23 at 0.3  $\mu\text{M}$  polymerized tubulin (100-fold excess). Note the stubs (arrows), presumably representing aggregated Tau, scattered along the MT wall at irregular intervals. The protofilaments are less visible than without Tau. The bar equals 50 nm.

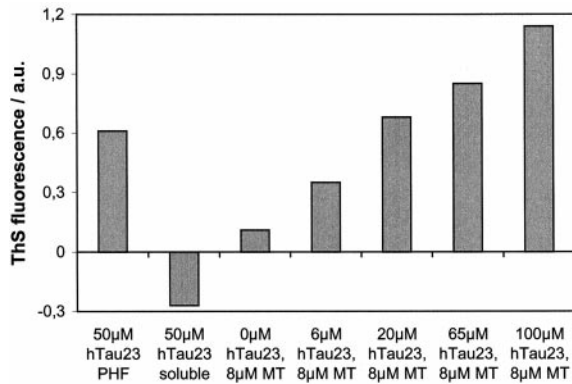


**FIG. 7. Interaction of Tau with MTs leads to ThS fluorescence.** All samples were incubated for 7 h at 37 °C in RB\* buffer (see “Materials and Methods”) and then exposed to 10  $\mu\text{M}$  thioflavin S. The bars represent the fluorescence after 30 min over the background of ThS alone (background). Note that in the presence of taxol-stabilized MTs (8  $\mu\text{M}$ ), the fluorescence correlates with the concentration of Tau. MTs alone (0  $\mu\text{M}$  hTau23, 8  $\mu\text{M}$  MT) or Tau alone (50  $\mu\text{M}$  hTau23, soluble) show only a small or even a negative fluorescence change. By comparison, Tau incubated with 8  $\mu\text{M}$  heparin (50  $\mu\text{M}$  hTau23, PHF) shows an enhanced fluorescence because of the formation of PHFs.

changes because of phosphorylation or mutations. Part of the discrepancies are presumably due to experimental procedures, such as the mode of titration or the method of determining bound and free Tau. For example, Butner and Kirschner (9) and Goode and Feinstein (12) used very low and fixed amounts of Tau (low nM range) and titrated against an excess of MTs (up to 40  $\mu\text{M}$ ); the bound Tau was detected by the radioactivity of incorporated  $^{35}\text{S}$ . Biernat *et al.* (10) and Gustke *et al.* (11) used fixed MT concentrations (30  $\mu\text{M}$ ), varied Tau in the  $\mu\text{M}$  range, and analyzed the fractions by quantifying SDS gels. Hong *et al.* (13) also varied Tau at fixed MTs, but at lower concentrations, and detection was done by radioactively labeled antibodies. In all these studies, the titrations appeared to confirm a simple binding behavior typical of independent ligand sites on a polymer, but the  $K_d$  values differed, and stoichiometries could be determined only in the latter three studies (where Tau was titrated against fixed MTs).

These problems of inconsistency lead us to suspect that perhaps the binding behavior of Tau was more complex than anticipated and that the concentration range and detection mode would have to be reconsidered. For this reason we developed an ELISA assay that allowed us to detect Tau over a wider

range of concentrations than before, and we repeated the earlier binding experiments, titrating Tau (up to 120  $\mu\text{M}$  total Tau) against different fixed MT concentrations (*e.g.* 3 or 20  $\mu\text{M}$ ). The results demonstrated that the binding shows at least two phases. The strong binding phase, visible at lower Tau concentrations, shows saturation behavior with dissociation constants in the 0.05–0.50  $\mu\text{M}$  range and stoichiometries around 0.2–0.3. This agrees well with the data of others (9, 12, 13), but the  $K_d$  is up to 10-fold lower than that reported by Gustke *et al.* (11). However, there is also a weaker binding phase that is remarkable because it cannot be saturated. The overloading parameter  $p$  (formally reminiscent of a  $K_d$  value if saturation is disregarded) reaches values around 50  $\mu\text{M}$ . This situation is in striking contrast to that of other MT-binding proteins such as motor proteins, which show saturable monophasic binding (52, 53), or for high molecular weight MAPs where cooperative binding has been reported (54, 55).

A consequence of the biphasic binding behavior is that the monophasic apparent binding parameters depend on limitations in the concentration range. Thus, our present ELISA data are in good agreement with the data obtained previously by densitometry of SDS gels (Fig. 4, *a* and *b*), but because the earlier interval of concentrations was too narrow, the interpretation in terms of one phase only lead to an overestimation of the  $K_d$  values and of stoichiometries.

How do modifications of Tau affect the binding parameters? We checked three types of modification that are important for the function of Tau, the repeat number, phosphorylation, and dimerization: (i) Tau isoforms contain three or four repeats in the C-terminal assembly domain that are thought to enhance the binding to MTs (9, 11, 56). This was confirmed with our new assay; four-repeat Tau (hTau40) binds six times more tightly than three-repeat Tau (hTau23) but with roughly the same stoichiometry (Table I). (ii) Phosphorylation tends to decrease the affinity (3, 10, 38, 57). This was also confirmed; phosphorylation at Ser<sup>214</sup> by PKA decreased the stoichiometry about 7-fold but left the  $K_d$  nearly unchanged. Thus, it appears that phosphorylated Tau effectively occupies a larger area on the MT surface. We note that in our hands only PKA and MARK have a strong effect on the Tau-MT interaction by phosphorylating Ser<sup>214</sup> in the flanking domain of the repeats or Ser<sup>262</sup> in the KXGS motifs of the repeats, whereas other kinases (such as proline-directed kinases) have only a moderate effect (10, 37). These were therefore not investigated further. (iii) Finally, the dimerization of Tau via cross-linking at Cys<sup>322</sup> is important because such dimers strongly enhance the aggregation into PHFs. We found a pronounced increase in affinity; dimers of hTau23 bind almost 10-fold more tightly and with almost double stoichiometry than monomers (Table I). Remarkably, both phosphorylation and dimerization affect the Tau-MT interaction in the same way as the Tau-Tau interaction leading to PHFs, *i.e.* phosphorylation inhibits both interactions, and dimerization promotes them (32). This strengthens the view that there is a structural relationship between the association of Tau with MTs and its PHF aggregation (see below).

**PHF-like State of Tau Bound to MTs?**—At elevated Tau concentrations the number of bound Tau molecules can greatly exceed the number of tubulin molecules (Fig. 4), let alone the number of high affinity binding sites (~25% of tubulin). This poses the question in which conformation Tau could accumulate on the MT surface. The issue may be of secondary importance in the physiological environment of a healthy cell where Tau is substoichiometric compared with tubulin (8). However, it may become relevant in a degenerating neuron in Alzheimer’s disease where on the one hand Tau becomes elevated, and on the other hand MTs decay (16). The reasons for the

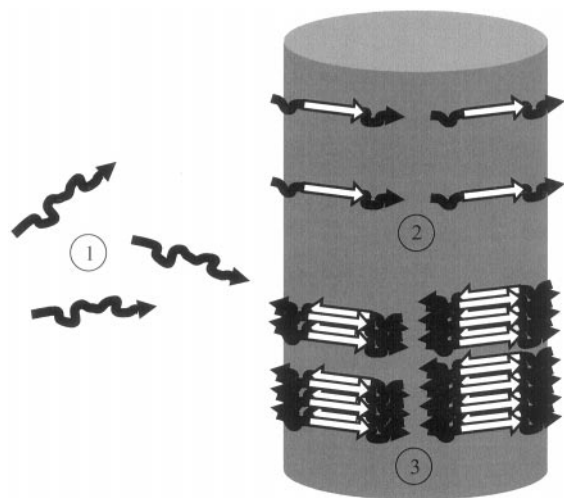


FIG. 8. **Model of Tau binding and accumulation on the MT surface.** 1, soluble Tau with a largely unfolded conformation. 2, initial binding of Tau to the MT surface (first phase of binding), accompanied by a conformational change. 3, further accumulation of Tau on the MT in a second nonsaturable binding phase, leading to an overloading of the MT surface.

aggregation of Tau into PHFs in an Alzheimer neuron are not well understood, but *in vitro* experiments show that the MT binding domain is involved (43), oxidation and formation of Tau dimers are important (33), and PHF aggregation is greatly accelerated by polyanionic molecules. The polyanions tested *in vitro* included mainly extracellular matrix components such as sulfated glycosaminoglycans, *e.g.* heparin or heparan sulfate (45, 46), polynucleotides such as RNA, or polycarboxylates such as acidic peptides, *e.g.* poly-Glu (47). It is not clear whether Tau interacts strongly with these substances in cells. RNA may be a candidate because Tau mRNA is transported into the proximal axon where Tau protein synthesis takes place (58). In addition, certain fractions of Alzheimer hyperphosphorylated Tau preparations can behave similar to polyanions in that they induce the aggregation of normal Tau (51).

However, a much more obvious polyanionic candidate is the C-terminal region of tubulin itself, exposed on the outer surface of MTs, which is unusually rich in Glu and Asp. Moreover, the charge can be potentiated by polyglutamylation (48, 49). In fact tubulin represents such a concentrated polyanion that one may ask why Tau does not normally form PHFs on the MTs. In physiologically normal conditions, the likely answer is that Tau is present only at low concentrations and is diluted over a large MT surface area. *In vitro*, the induction of PHFs by tubulin cannot be observed because the assembly of tubulin is dominant, *i.e.* Tau forces tubulin to assemble but not *vice versa*. Moreover, tubulin itself is in principle capable of self-nucleation and elongation above its critical concentration, even without Tau or other polycationic MAPs, whereas PHF aggregation *in vitro* requires polyanions not only for nucleation but also for elongation (29). Thus, even if a nucleus of PHFs was formed on the MT surface, it could not propagate into extended filaments unless the filaments propagate along the MTs because the polyanions (tubulin) are bound up in the form of MTs. But at least one would expect that Tau would show the signs of incipient PHF aggregation on the MT surface given the high negative charge. This is our interpretation of the ThS fluorescence signal (Fig. 7). The fluorescence increases characteristically when Tau aggregates into PHFs, even when different assembly inducers are employed, such as polyanions (22) or free fatty acids (59). ThS has some specificity for  $\beta$ -structure, which has recently been detected in the core of PHFs (60). No signal is observed with MTs alone nor with Tau alone when it does not

aggregate, but a signal develops with Tau aggregated into PHFs or with Tau bound to MTs. This means that (in terms of ThS binding and fluorescence) Tau adopts a state that is reminiscent of PHFs when it is adsorbed to the MT surface. The structure of this state is currently not known. One possibility is that of a Tau oligomer in a state of aggregation that resembles a PHF nucleus, as depicted in Fig. 8. This would be compatible with the small number of Tau molecules (about 10) that are sufficient for PHF nucleation in the presence of polyanions (29). If MTs decay in Alzheimer's disease neurons or if Tau becomes overexpressed, Tau could become overloaded on the MT surface, PHF nuclei could form, and eventually PHF elongation could take place right on the MT surface. This scenario suggests that tubulin could play an active role in the mechanism of pathological Tau aggregation.

**Acknowledgments**—We thank Heike Deisemann for excellent technical assistance and Dr. E.-M. Mandelkow for stimulating discussions and help with electron microscopy. The purified human Tau proteins were provided in part by Dr. J. Biernat.

#### REFERENCES

- Mandelkow, E., and Mandelkow, E. M. (1995) *Curr. Opin. Cell Biol.* **7**, 72–81
- Schoenfeld, T. A., and Obar, R. A. (1994) *Int. Rev. Cytol.* **151**, 67–137
- Bramblett, G. T., Trojanowski, J. Q., and Lee, V. M. (1992) *Lab. Invest.* **66**, 212–222
- Yoshida, H., and Ihara, Y. (1993) *J. Neurochem.* **61**, 1183–1186
- Ebneth, A., Godemann, R., Stamer, K., Illenberger, S., Trinczek, B., and Mandelkow, E. (1998) *J. Cell Biol.* **143**, 777–794
- Cleveland, D. W., Hwo, S. Y., and Kirschner, M. W. (1977) *J. Mol. Biol.* **116**, 227–247
- Cleveland, D. W., Hwo, S. Y., and Kirschner, M. W. (1977) *J. Mol. Biol.* **116**, 207–225
- Drubin, D., and Kirschner, M. (1986) *J. Cell Biol.* **103**, 2739–2746
- Butner, K. A., and Kirschner, M. W. (1991) *J. Cell Biol.* **115**, 717–730
- Biernat, J., Gustke, N., Drewes, G., Mandelkow, E. M., and Mandelkow, E. (1993) *Neuron* **11**, 153–163
- Gustke, N., Trinczek, B., Biernat, J., Mandelkow, E. M., and Mandelkow, E. (1994) *Biochemistry* **33**, 9511–22
- Goode, B. L., and Feinstein, S. C. (1994) *J. Cell Biol.* **124**, 769–782
- Hong, M., Zhukareva, V., Vogelsberg-Ragaglia, V., Wszolek, Z., Reed, L., Miller, B. I., Geschwind, D. H., Bird, T. D., McKeel, D., Goate, A., Morris, J. C., Wilhelmsen, K. C., Schellenberg, G. D., Trojanowski, J. Q., and Lee, V. M. (1998) *Science* **282**, 1914–1917
- Chau, M. F., Radeke, M. J., de Ines, C., Barasoain, I., Kohlstaedt, L. A., and Feinstein, S. C. (1998) *Biochemistry* **37**, 17692–17703
- Hiller, G., and Weber, K. (1978) *Cell* **14**, 795–804
- Khatoun, S., Grundke-Iqbal, I., and Iqbal, K. (1992) *J. Neurochem.* **59**, 750–753
- Panda, D., Goode, B. L., Feinstein, S. C., and Wilson, L. (1995) *Biochemistry* **34**, 11117–11127
- Goedert, M., Spillantini, M. G., and Davies, S. W. (1998) *Curr. Opin. Neurobiol.* **8**, 619–632
- Wilhelmsen, K. C. (1999) *Proc. Natl. Acad. Sci. U. S. A.* **96**, 7120–7121
- D'Souza, I., Poorkaj, P., Hong, M., Nochlin, D., Lee, V. M., Bird, T. D., and Schellenberg, G. D. (1999) *Proc. Natl. Acad. Sci. U. S. A.* **96**, 5598–5603
- DeTure, M., Ko, L., Yen, S., Nacharaju, P., Easson, C., Lewis, J., van Slegtenhorst, M., and Hutton, M. (2000) *Brain Res.* **853**, 5–14
- Friedhoff, P., Schneider, A., Mandelkow, E. M., and Mandelkow, E. (1998) *Biochemistry* **37**, 10223–10230
- Boucher, D., Larcher, J. C., Gros, F., and Denoulet, P. (1994) *Biochemistry* **33**, 12471–12477
- Maccioni, R. B., Vera, J. C., Dominguez, J., and Avila, J. (1989) *Arch. Biochem. Biophys.* **275**, 568–579
- Maccioni, R. B., Rivas, C. I., and Vera, J. C. (1988) *EMBO J.* **7**, 1957–1963
- Paschal, B. M., Obar, R. A., and Vallee, R. B. (1989) *Nature* **342**, 569–572
- Cross, D., Dominguez, J., Maccioni, R. B., and Avila, J. (1991) *Biochemistry* **30**, 4362–4366
- Brandt, R., Lee, G., Teplow, D. B., Shalloway, D., and Abdel-Ghany, M. (1994) *J. Biol. Chem.* **269**, 11776–11782
- Friedhoff, P., von Bergen, M., Mandelkow, E. M., Davies, P., and Mandelkow, E. (1998) *Proc. Natl. Acad. Sci. U. S. A.* **95**, 15712–15717
- Mandelkow, E. M., Herrmann, M., and Ruhl, U. (1985) *J. Mol. Biol.* **185**, 311–327
- Goedert, M., Spillantini, M. G., Jakes, R., Rutherford, D., and Crowther, R. A. (1989) *Neuron* **3**, 519–526
- Schneider, A., Biernat, J., von Bergen, M., Mandelkow, E., and Mandelkow, E. M. (1999) *Biochemistry* **38**, 3549–3558
- Schweers, O., Mandelkow, E. M., Biernat, J., and Mandelkow, E. (1995) *Proc. Natl. Acad. Sci. U. S. A.* **92**, 8463–8467
- Binder, L. I., Frankfurter, A., and Rehhun, L. I. (1985) *J. Cell Biol.* **101**, 1371–1378
- Bobrow, M. N., Harris, T. D., Shaughnessy, K. J., and Litt, G. J. (1989) *J. Immunol. Methods* **125**, 279–285
- McGhee, J. D., and Hippel, P. H. v. (1974) *J. Mol. Biol.* **86**, 469–489
- Illenberger, S., Zheng-Fischhofer, Q., Preuss, U., Stamer, K., Baumann, K.,

- Trinczek, B., Biernat, J., Godemann, R., Mandelkow, E. M., and Mandelkow, E. (1998) *Mol. Biol. Cell* **9**, 1495–1512
38. Drewes, G., Ebner, A., Preuss, U., Mandelkow, E. M., and Mandelkow, E. (1997) *Cell* **89**, 297–308
39. Amos, L. A. (1977) *J. Cell Biol.* **72**, 642–654
40. Zingsheim, H. P., Herzog, W., and Weber, K. (1979) *Eur J. Cell Biol.* **19**, 175–183
41. Voter, W. A., and Erickson, H. P. (1982) *J. Ultrastruct. Res.* **80**, 374–382
42. Hirokawa, N., Shiomura, Y., and Okabe, S. (1988) *J. Cell Biol.* **107**, 1449–1459
43. Wille, H., Drewes, G., Biernat, J., Mandelkow, E. M., and Mandelkow, E. (1992) *J. Cell Biol.* **118**, 573–584
44. Song, Y. H., and Mandelkow, E. (1993) *Proc. Natl. Acad. Sci. U. S. A.* **90**, 1671–1675
45. Perez, M., Valpuesta, J. M., Medina, M., Degarcini, E. M., and Avila, J. (1996) *J. Neurochem.* **67**, 1183–1190
46. Goedert, M., Jakes, R., Spillantini, M. G., Hasegawa, M., Smith, M. J., and Crowther, R. A. (1996) *Nature* **383**, 550–553
47. Kampers, T., Friedhoff, P., Biernat, J., and Mandelkow, E. M. (1996) *FEBS Letters* **399**, 344–349
48. Edde, B., Rossier, J., Le Caer, J. P., Desbruyeres, E., Gros, F., and Denoulet, P. (1990) *Science* **247**, 83–85
49. Westermann, S., Schneider, A., Horn, E. K., and Weber, K. (1999) *J. Cell Sci.* **112**, 2185–2193
50. Spillantini, M. G., and Goedert, M. (1998) *Trends Neurosci.* **21**, 428–433
51. Alonso, A. C., Grundke-Iqbal, I., and Iqbal, K. (1996) *Nat. Med.* **2**, 783–787
52. Hackney, D. D. (1994) *Proc. Natl. Acad. Sci. U. S. A.* **91**, 6865–6869
53. Thormahlen, M., Marx, A., Muller, S. A., Song, Y., Mandelkow, E. M., Aebi, U., and Mandelkow, E. (1998) *J. Mol. Biol.* **275**, 795–809
54. Wallis, K. T., Azhar, S., Rho, M. B., Lewis, S. A., Cowan, N. J., and Murphy, D. B. (1993) *J. Biol. Chem.* **268**, 15158–15167
55. Coffey, R. L., and Purich, D. L. (1995) *J. Biol. Chem.* **270**, 1035–1040
56. Coffey, R. L., Joly, J. C., Cain, B. D., and Purich, D. L. (1994) *Biochemistry* **33**, 13199–13207
57. Drechsel, D. N., Hyman, A. A., Cobb, M. H., and Kirschner, M. W. (1992) *Mol. Biol. Cell* **3**, 1141–1154
58. Litman, P., Barg, J., Rindzoonski, L., and Ginzburg, I. (1993) *Neuron* **10**, 627–638
59. King, M. E., Ahuja, V., Binder, L. I., and Kuret, J. (1999) *Biochemistry* **38**, 14851–14859
60. von Bergen, M., Friedhoff, P., Biernat, J., Heberle, J., and Mandelkow, E. (2000) *Proc. Natl. Acad. Sci. U. S. A.* **97**, 5129–5134
61. Zheng-Fischhöfer, Q., Biernat, J., Mandelkow, E. M., Illenberger, S., Godemann, R., and Mandelkow, E. (1998) *Eur. J. Biochem.* **252**, 542–552